Thessaloniki-GREECE 2007

4th International Conference on
Earthquake Geotechnical Engineering
June 25-28, 2007
Paper No. 1618

CENTRIFUGE MODEL TESTS ON ABUTMENT OF RIVER-CROSSING BRIDGE ON LIQUEFIABLE SOILS

Akihiro TAKAHASHI[1], Hideki SUGITA[2] & Shunsuke TANIMOTO[3]

ABSTRACT

Earthquake-induced deformation of a bridge abutment can be large when the bridge is built on liquefiable ground and crosses a water channel. As seismic response of a bridge abutment on liquefiable ground is the consequence of complex interactions among the bridge, abutment and surrounding soils, identification of the factors dominating the abutment response is important for simplified seismic design methods. This paper reports the results of dynamic centrifuge model tests on bridge abutments adjacent to a river dike, including consideration of liquefaction of the underlying ground. The test results demonstrate importance of considerations of the softening of the soil in the layer beneath the liquefiable layer during earthquake and geometry of the ground surrounding the abutment in examination of seismic piled abutment performance.

Keywords: Abutment, Centrifuge model test, Liquefaction, Pile foundation

INTRODUCTION

Earthquake-induced deformation of a bridge abutment can be large when the bridge is built on a floodplain or reclaimed area, i.e., liquefiable ground, and crosses a water channel. When the abutment is located adjacent to a river dike or revetment, it is especially prone to movement toward the waterfront during an earthquake when the underlying ground liquefies.

In conventional design methods (e.g., JRA 2002), the seismic performance of bridge abutments on liquefiable soil is assessed by calculating the response of the abutment subjected to (1) the inertial force of the superstructure and the abutment, and (2) the seismic active earth pressure of the backfill. The kinematic load induced by interaction between the surrounding soils and structure have been neglected, for simplicity because liquefaction of the foundation soil appears to cause a reduction of lateral soil resistance (Shirato et al., 2006.) Although the seismic performance of abutments is affected by (1) local deformation of the adjacent river dike, (2) deformation of foundation soils caused by the weight of a road embankment connected to the abutment, and (3) slumping of the road embankment itself, these are seldom considered in the conventional design methods. Because the seismic response of a bridge abutment on liquefiable ground is the consequence of complex interactions among all these factors, identifying the factors dominating the abutment response is critical when simplified seismic design is used.

This paper reports the results of dynamic centrifuge model tests on bridge abutments built on liquefiable ground adjacent to river dikes. Observed responses of a typical abutment of a river-crossing bridge are firstly described in detail. Subsequently comparisons of the abutments responses for three different geometries of the surrounding ground are made to examine how earthquake-induced deformations of the surrounding soils affect the seismic responses of bridge abutments.

[1] Senior Researcher, Public Works Research Institute, Japan, Email: aki-taka@pwri.go.jp.
[2] Team Leader, Public Works Research Institute, Japan, Email: sugita@pwri.go.jp.
[3] Researcher, Public Works Research Institute, Japan, Email: s-tanimo@pwri.go.jp.

Table 1. Properties of soils used

Layer	Soil	D_{50} (mm)	Dry density (kN/m^3)
Loose sand layer, including surface layer and fills above water table	Edosaki sand	0.25 (*Fc*=8.2%)	13.2
Dense sand layer	Toyoura sand	0.18	15.4
Bearing stratum	Toyoura sand	0.18	16.0

CENTRIFUGE MODEL TEST PROCEDURES AND CONDITIONS

Highway bridge abutments constructed near a river channel were modelled. Three configurations of the ground surrounding the abutment were considered; a plan view and cross section of the models are illustrated in Fig. 1. The tests were conducted at 50g with application of earthquake motion in the bridge axis direction. In the modelling, taking the advantage of symmetry, only half width of the abutments was modelled, and prototype scales of all dimensions of the model are reduced to half of those for a typical bridge abutment due to the limitations of the container size, i.e., shake table tests were performed on 1/100 models at 50g.

The pile foundation was modelled with nine 10mm-diameter stainless steel pipe piles (EI=11N.m^2), arranged in 3x3 grids (6x3 for full width) with 25mm spacing. The model abutment was made of aluminium. The width of the bridge was 150mm (only half width was modelled in the physical model tests), and the slopes of the river dike and road embankment connected to the 90mm-high pile-supported abutment were 1V: 2H and 1V: 1.8H, respectively. The water level was set at 90mm below the crest of the dike. The original ground level was 50mm above riverbed for the cases illustrated in Fig. 1(a)(c), and was 115mm for the case shown in Fig. 1(b). The thickness of the liquefiable layer (loose sand deposit) below the water table was 115mm. The piles were installed in three layers: a bottom bearing stratum, a non-liquefiable layer (dense sand deposit), and the liquefiable layer. Properties of soils used are listed in Table 1.

Figure 2 shows the applied earthquake motions. The inland earthquake motion (Step 1) was applied to the models followed by the near-land inter-plate earthquake motion (Step 2.) At least an interval of 10 minutes (approx. 8 hours in prototype scale) was allowed between the applications of shaking to make sure that dissipation of the excess pore water pressure completed before Step 2 shaking was applied. The earthquake motions were applied in the bridge axis direction. Three physical model tests were performed for the models shown in Fig. 1. For the cases with the lower original ground level (Cases 1 & 3), water-ward and landward stretching of the river dike and the slumping of the road embankment were expected. In the case with the higher ground level (Case 2), because the original ground level was set to a height of the ground level of the roadway, the expected deformation mode of the surrounding ground was simpler than that for the other cases. By comparing Cases 1 and 2, the effect that the surrounding ground geometry has on the seismic response of the abutment can be observed. In Case 3, as the ordinary waterway is distant from the abutment, different deformation mode of the surrounding soils from Case 1 is expected.

The limitations in the physical model tests are: (1) the bridge deck was not modelled, and (2) the abutment top was free to move, without restriction, i.e., the “strut effect” of the bridge deck on abutment response was not modelled. In other words, the dynamic interaction between the deck and the abutment was not modelled, because our main concern was the interaction between the abutment, foundation ground, road embankment, and river dike. Because of these limitations, the observed deformations and vibration modes of the abutment may have been different from those in a real bridge-foundation system.

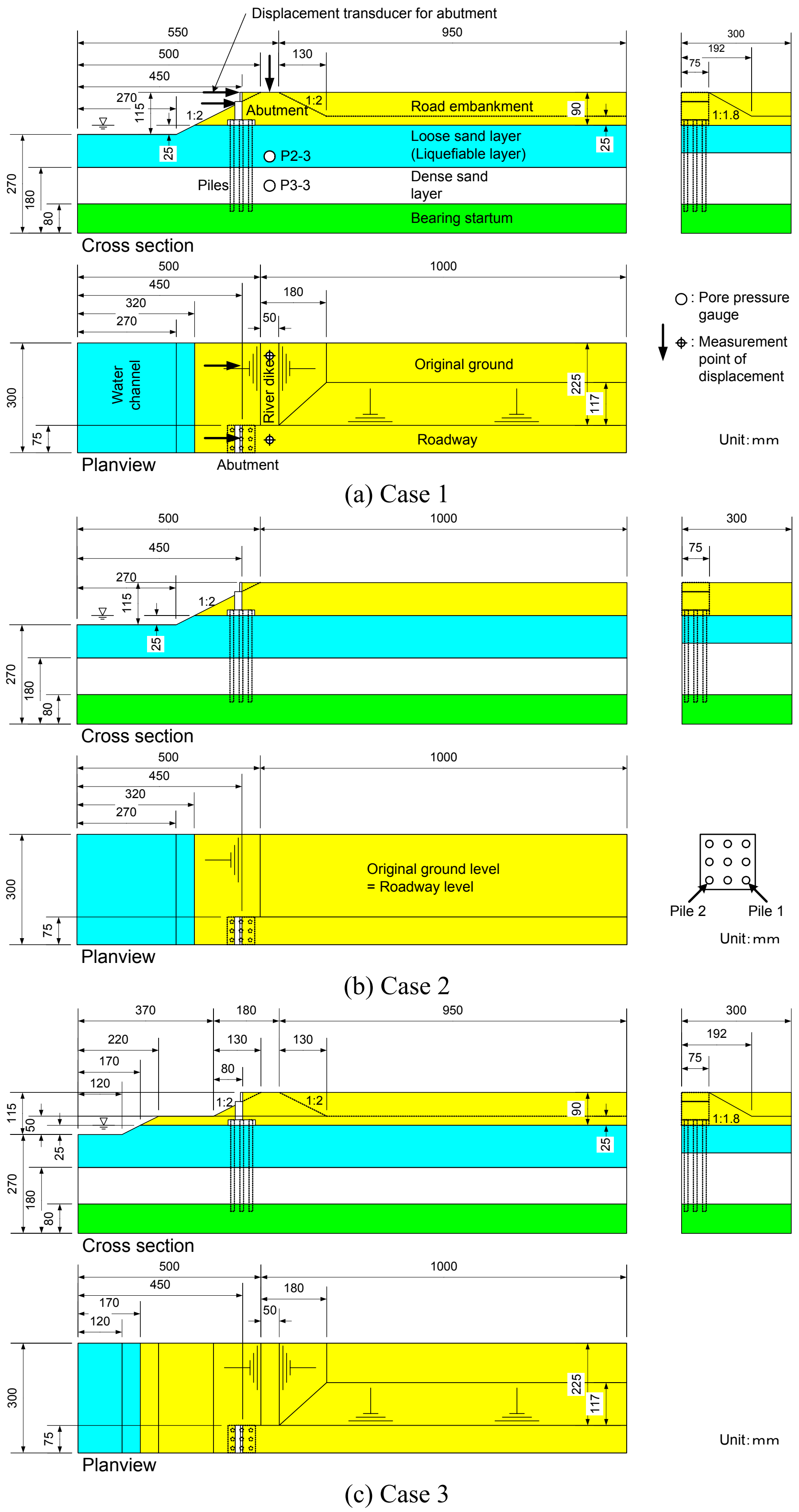

Figure 1. Centrifuge model packages

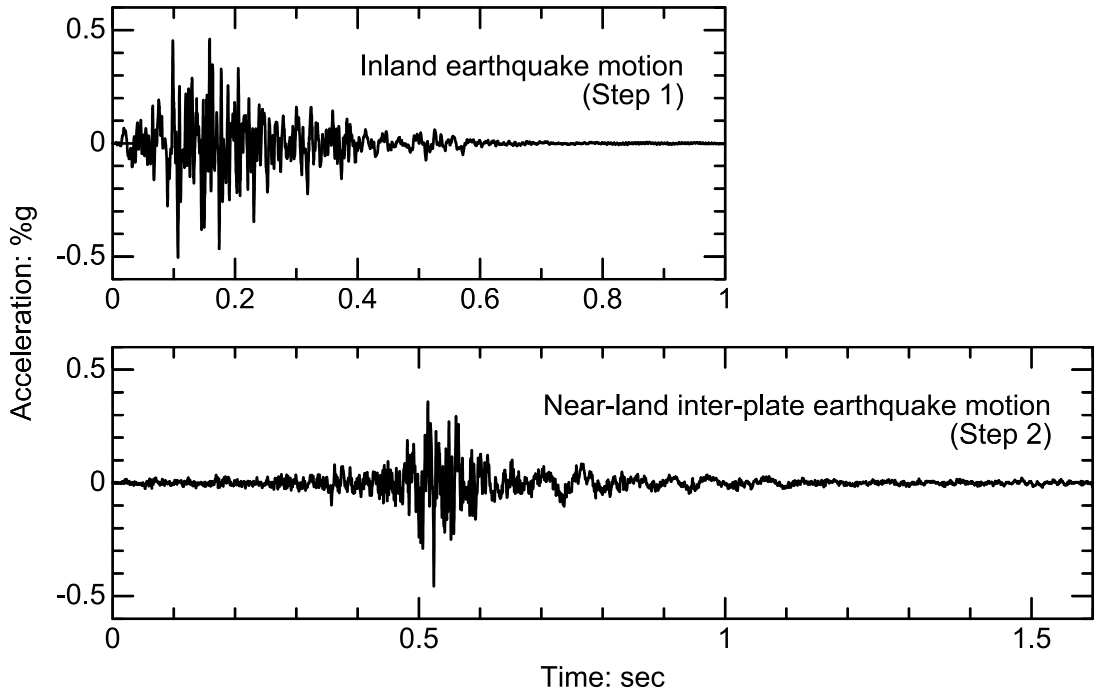

Figure 2. Earthquake motions applied

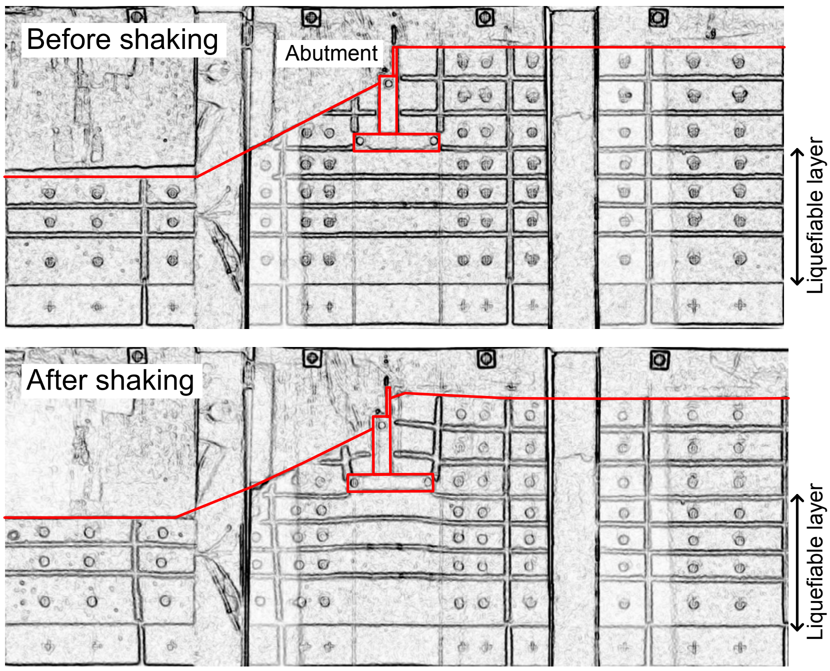

Figure 3. Side views of the model ground before and after shaking (Case 1)

TEST RESULTS AND DISCUSSION

Responses of abutment for the reference case (Case 1) are firstly presented. Subsequently comparisons of the abutments responses for three different geometries of the surrounding ground are made.

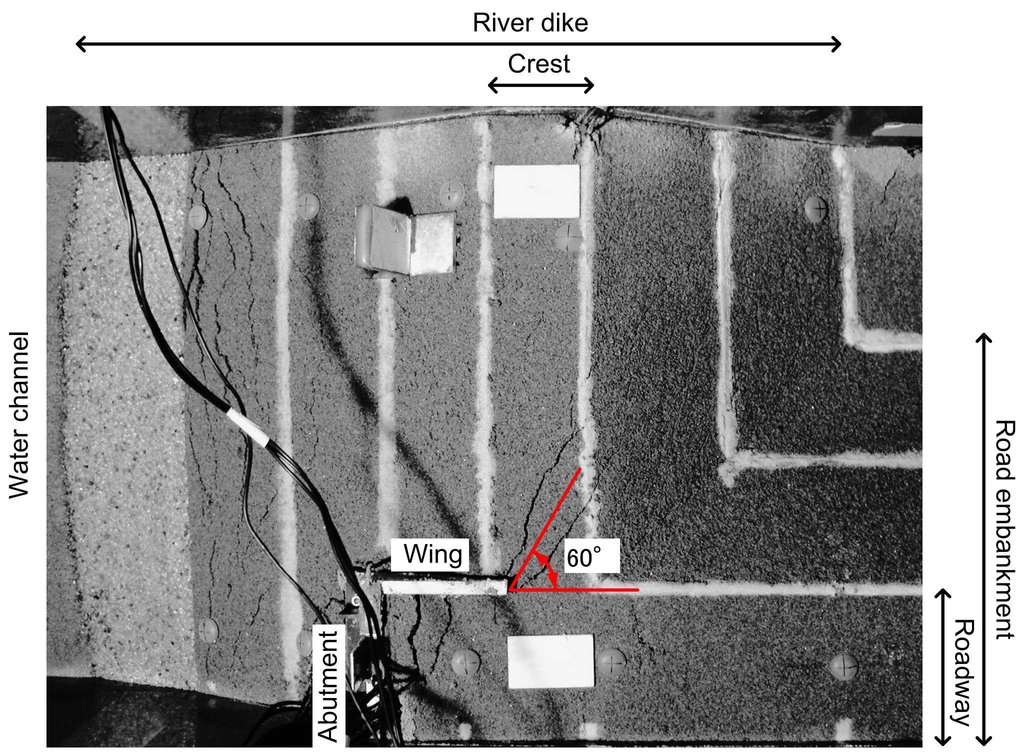

Figure 4. Top view of model ground after shaking (Case 1)

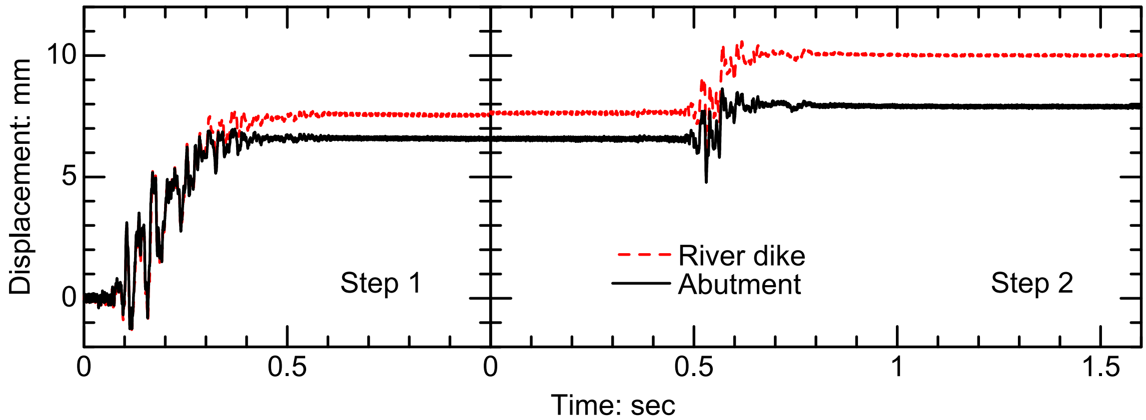

Figure 5. Time histories of horizontal displacements of abutment and river dike (Case 1)

Responses of abutment in river dike

Deformation of soils surrounding abutment

Side views of the model ground before and after shaking are illustrated in Fig. 3 for Case 1. The slope of the river dike in front of the abutment moved toward the water channel and the underlying liquefiable soil showed large shear deformation during earthquake, resulting in large horizontal displacement of the abutment. Subsidence of the road embankment connected to the abutment was also observed. This was due to (1) the waterward displacement of the abutment, (2) stretching of the road embankment perpendicular to the bridge axis, and (3) volume change of the loose sand deposit under the embankment.

Figure 4 shows the top view of the ground surface after shaking for Case 1. Since the piled abutment restrained the liquefaction-induced horizontal deformation of the river dike toward the water channel, the horizontal deformation of the river dike around the abutment was smaller than that far from the

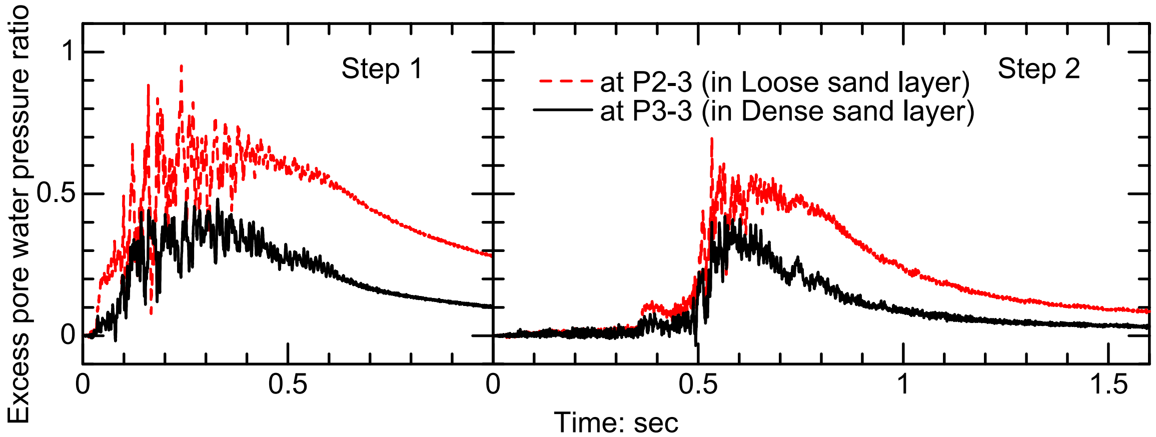

Figure 6. Time histories of excess pore water pressure ratio (Case 1)

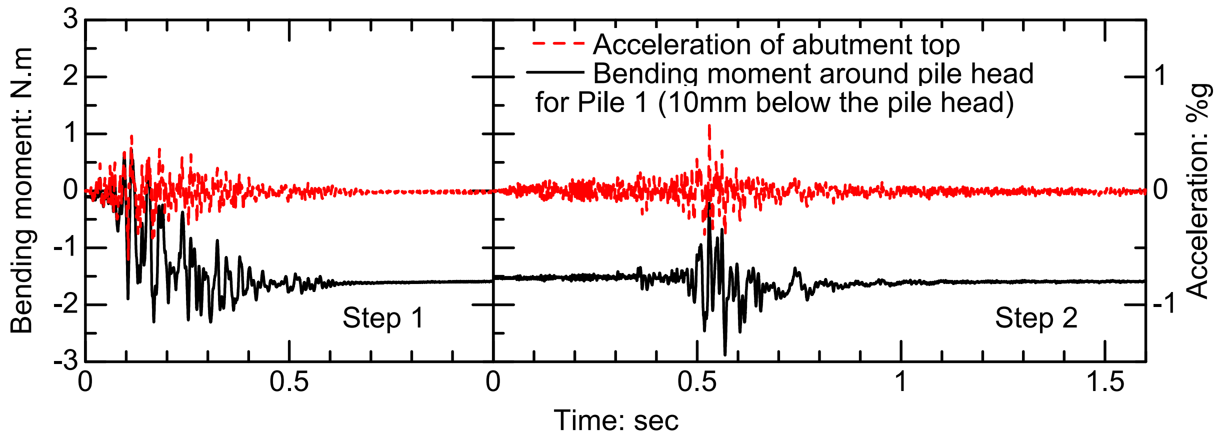

Figure 7. Time histories of horizontal acceleration of abutment top and bending moment around pile head (Case 1)

abutment. This difference caused propagation of the crack at the crest of the river dike from the edge of the abutment wing.

Abutment displacement

Time histories of horizontal displacements of abutment and river dike are shown in Fig. 5. In Step 1 evolution of the horizontal displacement of the abutment was almost identical to that of the water-channel-side slope of the river dike during the first half of the main shock. Relative horizontal displacement of the abutment and river dike got larger in the last half of the main shock in Step 1 and Step 2.

Figure 6 plots time histories of the excess pore water pressure ratio measured near the pile foundation of the abutment for Case 1. Locations of the pressure gauges are indicated by circles in Fig. 1. Here the excess pore water pressure ratio is defined as a ratio of the excess pore water pressure to the estimated initial vertical effective stress. In Step 1, the excess pore water pressure in the loose sand layer reached a certain value around t=0.2sec and levelled off, followed by dissipation starting around t=0.4sec. Due to the initial shear stress in the soil around the abutment, no full liquefaction took place at the measured point (P2-3.) In the dense sand layer, the maximum value of the excess pore water pressure ratio reached 0.4 and was far from the liquefaction.

Comparison of the evolution of the horizontal displacement of the abutment to the excess pore water pressure responses reveals that accumulation of the horizontal displacement of the abutment stopped

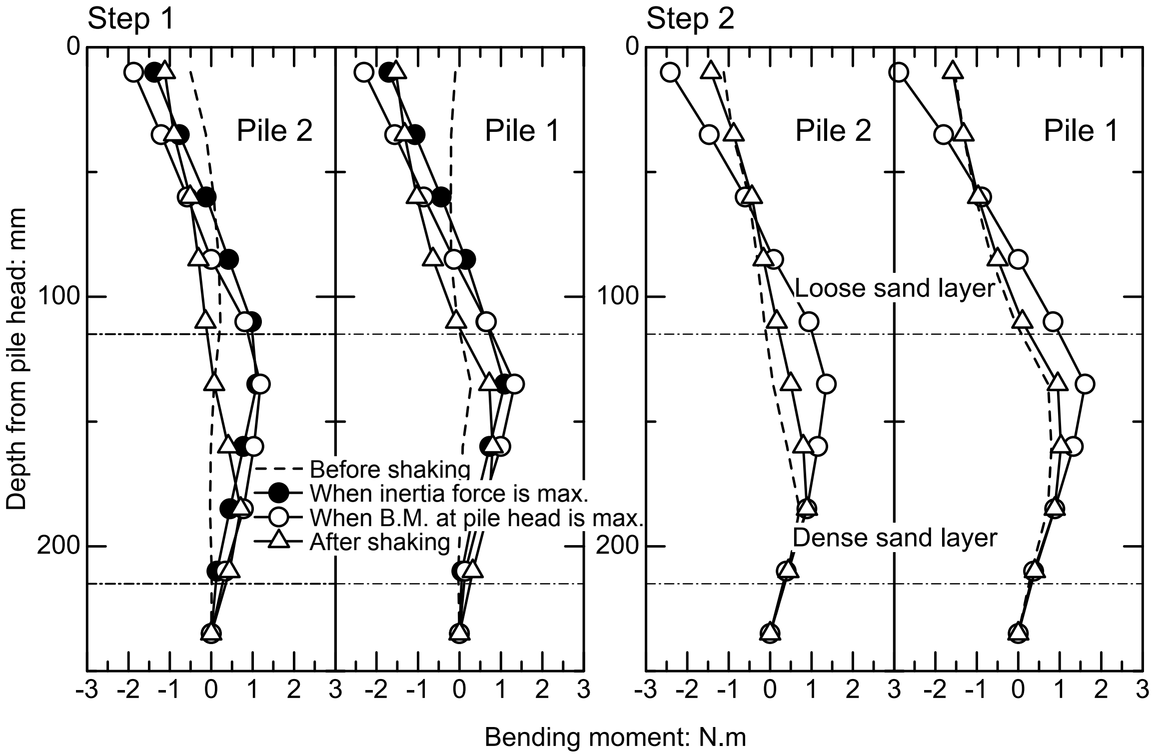

Figure 8. Bending moment distributions of piles (Case 1)

when the excess pore water pressure started dissipating at the non-liquefiable layer, i.e., dense sand layer (t=0.3sec in Step 1 and t=0.6sec in Step 2.) This fact indicates that the permanent horizontal displacement of the abutment is affected by the softening of the soil in the layer beneath the liquefiable layer and suggests that importance of the consideration of such effect in examination of permanent displacement of the piled abutment.

Bending moment of piles

Time histories of the horizontal acceleration of the abutment top and bending moment around pile head for Pile 1 (whose location is shown in Fig. 1(b)) are shown in Fig. 7 for Case 1. The maximum bending moment throughout shaking was observed around the pile head in all the cases. In both the shaking steps, the maximum abutment acceleration, i.e., the maximum inertia force of the abutment, was observed (t=0.11sec for Step 1 and t=0.53sec for Step 2) well before appearance of the largest bending moment (t=0.16sec for Step 1 and t=0.57sec for Step 2.)

Bending moment distributions at the relevant times are plotted in Fig. 8 for Case 1. The locations of the pile are shown in Fig. 1(b). Comparisons of the bending moment distributions before and after shaking reveal that (1) the permanent deformation of the river dike surrounding the piles imposed large deformation of the piles in Step 1, but (2) such large changes could not be observed in Step 2 even though increase of the permanent displacement of the abutment was seen in the step. In any case the final distributions of the pile bending moment exhibit two features; (1) the local maximum point is located just below the interface between the loose and dense sand layers and the bending moment distribution in the loose sand layer is concave upwards in Pile 1 (the pile in the road embankment-side row,) while (2) the local maximum point other than the pile head is very deep (just above the interface between the dense sand layer and bearing stratum) in Pile 2 (the pile in the water channel-side row.) The former indicates that the piles in the road embankment-side row were subjected to the force toward the water channel in the loose sand layer, i.e., so-called "lateral spreading force" in such as the NCHRP 472 Recommended Specifications for Seismic Design of Bridges (TRB 2002, Martin et al. 2002,) at the end of shaking, even though this was not relevant during the principal shock as described subsequently. For the latter, reduction of soil resistance at the dense sand layer due to the large

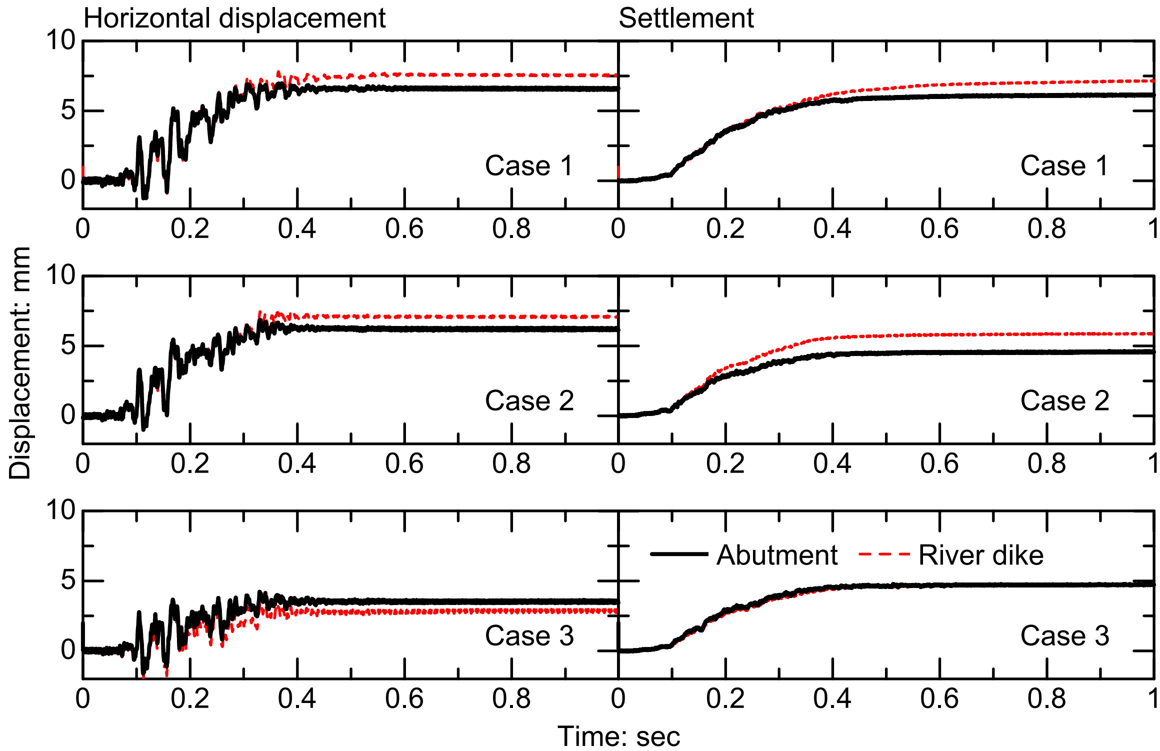

Figure 9. Time histories of horizontal displacement and settlement of abutment and river dike

waterward deformation of the slope in front of the abutment and the penetration of the piles in the water channel-side row may have resulted in the deformation mode of the piles mentioned above.

The bending moment distributions at the time of the maximum inertia force of the abutment (plots with the filled circles in Step 1) were very similar to those for the maximum bending moment being observed at the pile head (plots with the open circles in Step 1.) In addition to this, at these times, the bending moment distributions in the loose sand layer were almost straight, i.e., there was no marked soil reaction in the layer. These facts indicate that (1) the force dominated the piles response was the inertia force of the abutment (and perhaps the earth pressure acting on the abutment) and (2) the loose sand layer showed little soil resistance and the horizontal force from the pile head was mainly supported by the dense sand layer at these times. Probably continuous increase of the excess pore water pressure at the dense sand layer after the arrival of the maximum inertia force of the abutment (see Fig. 6) softened the dense sand layer and hence the maximum bending moment at the pile head did not coincide with the maximum inertia force of the abutment. This again demonstrates importance of the consideration of the softening of the soil in the layer beneath the liquefiable layer in examination of seismic piled abutment performance.

Comparisons of abutment responses for three different surrounding ground geometries

Figure 9 shows time histories of the horizontal displacement and settlement of the abutment and river dike in Step 1 for all the cases. Locations of measurement point are shown in Fig. 1(b). As expected, in Case 3 where the ordinary waterway was distant from the river dike, the soil in front of the river dike behaved as a counterweight fill and made the horizontal displacement of the river dike as well as that of the abutment smaller.

However, the horizontal displacements of the abutment and river dike in Cases 1 and 2 (the original ground level is low in the former while that is the same as the river dike crest for the latter) are surprisingly comparable. In three-dimensional finite element analyses on a similar bridge abutment (Takahashi et al., 2006 & 2007,) due to the landward stretching of the river dike and the relatively smaller earth pressure acting on the abutment, the horizontal displacements of the abutment and river dike were much smaller for the case with the lower original ground level (corresponding to Case 1 in this study). Possible reasons for the difference between the physical and numerical modelling may be; (1) length of the modelling domain normal to the bridge axis was much smaller in the physical model test and (2) stiffness of the soil above water table in the physical model test may have been larger than that in the numerical analyses.

For the settlement of the abutment backfill and river dike crest, similar trends to the horizontal displacement were observed, except the settlements for Case 2. (In this case, the settlements were smaller than those for Case 1 as expected from the geometry difference.) Further data processing and analysis are needed to make comparisons of the abutment responses for the three different surrounding ground geometries in detail.

SUMMARY

This paper reports the results of dynamic centrifuge model tests on bridge abutments built on liquefiable ground adjacent to river dikes. The test results demonstrate importance of considerations of the softening of the soil in the layer beneath the liquefiable layer during earthquake and geometry of the ground surrounding the abutment in examination of seismic piled abutment performance. None of these are explicitly considered in the conventional design methods for abutments, it is recommended to consider these two factors in the abutment design when the performance examinations are made in terms of displacements.

REFERENCES

Japan Road Association. 2002. Specifications for road bridges, Part V, Seismic Design, 333pp.

Martin, G.R., March, M.L., Anderson, D.G., Mayes, R.L. & Power, M.S. 2002. Recommended design approach for liquefaction induced lateral spreads, Proc. 3rd National seismic Conference and workshop on bridges and highways, MCEER-02-SP04, Buffalo, NY.

Shirato, M., Fukui, J. & Koseki, J. 2006. Current status of ductility design of abutment foundations against large earthquake, Soils and Foundations, Vol.46, No.3, 377-396.

Takahashi, A., Sugita, H. & Tanimoto, S. 2006. Behaviour of piled bridge abutment on liquefiable soils, Proceedings of 3rd International Conference on Urban Earthquake Engineering, Yokohama, Japan, 95-102.

Takahashi, A., Sugita, H. & Tanimoto, S. 2007. Forces acting on bridge abutments over liquefied ground, Accepted for publication in Soil Dynamics and Earthquake Engineering as of 22 December 2006.

Transportation Research Board, National Research Council. 2002. Comprehensive specification for the seismic design of bridges, National Cooperative Highway Research Program, Report No.472, National Academy Press.